

Density functional characterization of the antiferromagnetism in oxygen-deficient anatase and rutile TiO₂

Kesong Yang,^{a,b} Ying Dai,^{a,*} Baibiao Huang,^a and Yuanping Feng,^{b†}

^a *School of Physics, State Key Laboratory of Crystal Materials, Shandong University, Jinan 250100, People's Republic of China*

^b *Department of Physics, National University of Singapore, 2 Science Drive 3, Singapore 117542*

We present theoretical evidence for local magnetic moments on Ti³⁺ ions in oxygen-deficient anatase and rutile TiO₂ observed in a recent experiment [S. Zhou, et al., Phys. Rev. B **79**, 113201 (2009)]. Results of our first-principles GGA+U calculations reveal that an oxygen vacancy converts two Ti⁴⁺ ions to two Ti³⁺ ions in anatase phase, which results in a local magnetic moment of 1.0 μ_B per Ti³⁺. The two Ti³⁺ ions, however, form a stable antiferromagnetic state, and similar antiferromagnetism is also observed in oxygen-deficient rutile phase TiO₂. The calculated results are in good agreement with the experimentally observed antiferromagnetic-like behavior in oxygen-deficient Ti-O systems.

PACS number(s): 75.50.Pp; 75.50.Ee; 71.15.Mb

Owing to their promising applications in the spintronics, numerous attempts have been made to prepare diluted magnetic semiconductors (DMS) by doping semiconductors, particularly transition metal oxides TiO_2 and ZnO , with magnetic ions.^{1, 2} Recently, high-temperature ferromagnetism was found in one class of semiconductors without magnetic ion dopants,^{3,4} which is referred to as the d^0 magnetism.⁵ For example, ferromagnetism was observed in undoped HfO_2 consisting of nonmagnetic ions Hf^{4+} (d^0) and O^{2-} ,⁴ for which electronic structure calculations showed that the local magnetic moments produced by the Hf vacancies are ferromagnetically coupled.⁶ Room-temperature ferromagnetism was also reported in other undoped semiconductors such as In_2O_3 , SnO_2 , and TiO_2 .⁷⁻¹⁰ Among the various oxides, magnetic property of undoped TiO_2 has been widely studied.⁹⁻¹² However, despite of numerous studies, the origin of the ferromagnetism in undoped TiO_2 remains unclear. Both oxygen vacancy and titanium vacancy were proposed to be responsible for the ferromagnetism. On one hand, theoretical studies indicated that the cation vacancy or divacancy are ferromagnetically coupled,^{13,14} similar to the case of undoped HfO_2 .⁶ But on the other hand, more and more experimental evidences show that the magnetic property of undoped TiO_2 is strongly related to oxygen vacancy, and thus it was thought to be the source of room-temperature ferromagnetism in undoped semiconducting or insulating oxides.^{7, 10-12} Although the electronic state induced by the oxygen vacancy has been studied by first-principles theoretical calculations,^{15, 16} few works have been focused on its magnetic property. In particular, a recent experiment reported the presence of Ti^{3+} ions in rutile phase at the substitutional sites near oxygen vacancies, and the unpaired $3d$ electron of the Ti^{3+} (d^1) ion provides the local magnetic moment.¹⁷ Consequently, an interesting question occurs to us:

how do the local magnetic moments of the Ti^{3+} ions interact, and whether the coupling is ferromagnetic or antiferromagnetic. Since oxygen vacancies are very common in oxides, it would be useful to clarify the influence of oxygen vacancy on the magnetic property of undoped TiO_2 .

In this work, we investigate magnetic property of oxygen-deficient anatase and rutile TiO_2 by first-principles GGA+U electronic structure calculations. We find that owing to the charge imbalance created by the oxygen vacancy, two excess electrons occupy the localized 3d orbitals of the nearest neighbor Ti, thereby converting two Ti^{4+} ions to two Ti^{3+} ions in anatase phase, each with a local magnetic moment of $1.0 \mu_B$. However, the two Ti^{3+} ions form a stable antiferromagnetic configuration, and similar antiferromagnetism is also found in rutile TiO_2 .

Our spin-polarized GGA+U electronic structure calculations are carried out using the Vienna *ab initio* simulation package.^{18, 19} Oxygen-deficient anatase and rutile models are constructed by removing an oxygen atom from 48-atom $2 \times 2 \times 1$ anatase supercell and 72-atom $2 \times 2 \times 3$ rutile supercell, respectively. Projector augmented wave (PAW) potentials are used to describe the electron-ion interaction while the generalized gradient approximation (GGA) parameterized by Perdew and Wang (PW91) is used for electron exchange-correlation functional.²⁰ The cut-off energy of 400 eV and a $2 \times 2 \times 2$ k-point set centered at Γ point are sufficient to converge the total energy to within a tolerance of 10^{-6} eV. The lattice parameters and all the atomic positions are fully optimized until all components of the residual forces are smaller than $0.01 \text{ eV}/\text{\AA}$. In our GGA+U calculations, the on-site effective U parameter ($U_{\text{eff}}=U-J = 5.8 \text{ eV}$) proposed by Dudarev *et al.*²¹ is adopted for Ti 3d electron,²² which is in

agreement with the optimal U value (5.5 ± 0.5 eV).²³

The total density of states (TDOS) plots of oxygen-deficient anatase and rutile TiO₂ are presented in **Fig. 1** and **Fig. 2**, respectively. For oxygen-deficient anatase phase, the calculated results show that the TDOS is spin-unpolarized, and some defect states are localized in the band gap. Interestingly, the partial density of states (PDOS) of the two Ti ions around the oxygen vacancy given in **Figs. 1b** and **1c**, respectively, are spin polarized. However, their magnetic moments are in opposite directions, which results in a zero total magnetic moment. In contrast, the PDOS of the third nearest neighbor Ti ion of the oxygen vacancy does not show any spin polarization, as shown by the following spin density distribution of **Fig. 4a**. This indicates that the two electrons introduced by the neutral oxygen vacancy are captured by the two neighboring Ti ions, forming two T³⁺ ions with a local spin magnetic moment of $1.0 \mu_B$. This, however, is in contrast to results of a recent theoretical study based on the local spin density approximation (LSDA), in which the authors suggested that the oxygen vacancy does not produce any magnetic moments.¹⁴ This discrepancy could be due to the fact that the standard DFT calculations in the scheme of either local density approximation (LDA) or generalized gradient approximation (GGA) cannot treat properly the strong Coulomb interaction between 3d electrons, and thus may lead to an inadequate description of 3d states of Ti³⁺ in the oxygen-deficient TiO₂ system. As in the case of oxygen-deficient anatase TiO₂, some localized band gap states introduced by the oxygen vacancy are also found in oxygen-deficient rutile phase of TiO₂ through GGA+U calculations (see **Fig. 2**), and the further PDOS (**Figs. 2b** and **2c**) indicates that these localized impurity states consist of the spin-polarized states of Ti ions around the oxygen vacancy. In rutile phase, in contrast with

anatase phase, the electronic states of the three Ti ions around the oxygen vacancy are both spin-polarized, and the calculated PDOS for two equivalent Ti ions is down-spin, and the third one is up-spin, which leads to a total spin magnetic moment of zero. This result can be clearly reflected by the following spin density distribution plot of **Fig. 4b**. This suggests that one Ti^{4+} ion is reduced to a Ti^{3+} with a spin magnetic moment of $1.0 \mu_B$, while the other two Ti^{4+} ions share one remaining electron introduced by oxygen vacancy and hence are reduced into low-state Ti ions (close to +3.5), respectively. The different electron states of these Ti ions also lead to different impurity level positions in the band gap, as shown in **Fig. 2**. The different electronic distribution on the adjacent Ti ions around the oxygen vacancy in oxygen-deficient anatase and rutile TiO_2 can be explained by their different local geometrical structures. In **Fig. 3**, we plot the local structures of oxygen-deficient anatase and rutile TiO_2 models, respectively. In anatase phase, after geometrical optimization, the distance between the two equivalent Ti ions and the oxygen vacancy (marked as yellow color in **Fig. 3a** and labeled as Ti-V_O bond in the following discussion for convenience) are smaller than the third Ti-V_O bond (marked as green color in **Fig. 3a**) (1.950 vs. 2.03 \AA), and thus the two electrons introduced by the oxygen vacancy will occupy the two equivalent Ti ions preferredly, producing a magnetic moment of $1.0 \mu_B$ on each Ti ion with opposite spin directions. In contrast, in rutile phase, upon structural relaxation, two equivalent Ti-V_O bonds (marked as yellow color in **Fig. 3b**) are longer than the third Ti-V_O bond (marked as green color in **Fig. 3b**). As a result, one of the two electrons induced by the oxygen vacancy will firstly occupy the nearest Ti ion, which reduces the Ti^{4+} to Ti^{3+} with a spin magnetic moment of $1.0 \mu_B$, and the other electron was captured by the two equivalent Ti^{4+} ions and forms a total magnetic

moment of $1.0 \mu_B$ with opposite spin direction. In conclusion, these calculated results provide a clear theoretical evidence for experimentally observed Ti^{3+} ions in oxygen-deficient rutile TiO_2 .¹⁷

To further investigate the magnetic coupling characteristic between the local moments from the induced Ti^{3+} ions by oxygen vacancy in anatase and rutile TiO_2 , we compared the total energies of ferromagnetic and antiferromagnetic alignments of the magnetic moments on the generated Ti^{3+} ions. It is found that the antiferromagnetic state is more stable than the ferromagnetic state by 474 meV for anatase phase TiO_2 , and by 175 meV for rutile phase TiO_2 . For anatase phase, we repeated our calculation using a 96-atom $2 \times 2 \times 2$ supercell in which two oxygen vacancies were separated by the distance about 7.6 Å. The antiferromagnetic alignment of the two Ti^{3+} ions around each oxygen vacancy remains more energetically favorable compared to the ferromagnetic alignment. The calculated results are in good agreement with the experimentally observed antiferromagnetic-like behavior in oxygen-deficient Ti-O system.²⁴

To understand the nature of spin exchange coupling in oxygen-deficient anatase and rutile TiO_2 , we show their spin density distributions under antiferromagnetic alignment in **Figs. 4a** and **4b**, respectively. In anatase phase, the spin density is mainly distributed on the two Ti^{3+} ions and they have opposite spin directions. In contrast, in rutile phase, the two equivalent Ti ions share one electron introduced by oxygen vacancy and thus they have the same spin direction, and the third Ti^{3+} (d^1) ion possesses the one remaining electron, which provides a magnetic moment of $1.0 \mu_B$ with opposite spin direction. It is well-known that the superexchange model was widely used to explain the antiferromagnetic coupling between two

next-nearest neighbor cations through a non-magnetic anion (MnO, FeO, etc.).²⁵ However, in the oxygen-deficient TiO₂ model, the middle non-magnetic oxygen atom is removed, and thus the classical superexchange mechanism is not appropriate to explain the antiferromagnetism in this model. Therefore, in light of the information obtained from the first-principles calculations, we propose another possible superexchange model on the basis of the indirect *d-d* hopping between the paired Ti³⁺ ions via the adjacent Ti⁴⁺, as illustrated in **Fig. 5**, to explain the AFM coupling in oxygen-deficient TiO₂. The electron in each Ti³⁺ (*d¹*) ion hops to the *d* orbital of the adjacent Ti⁴⁺ through the oxygen ions, making the Ti⁴⁺ ion a low-spin Ti²⁺ (*d²*) state. In this process, the electrons do not have to change their spin directions, and thus the overall energy saving can lead to an antiferromagnetic alignment of the two Ti³⁺ ions.

As a comparison, we also investigated the electronic and magnetic property of titanium-deficient anatase TiO₂. Similar to the case of HfO₂⁶ and CaO²⁶, the presence of cation vacancy causes a clear spin split in the valence band, and a total magnetic moment of 4.0 μ_B was produced, mainly contributed by the six adjacent oxygen ions around the titanium vacancy which is consistent with results of previous calculations based on LSDA or GGA functional.^{13, 14} Further calculations were carried out to assess the relative stability of the ferromagnetic and antiferromagnetic alignments between the magnetic moments localized on different titanium vacancies using the 96-atom $2 \times 2 \times 2$ supercell where the distance between two titanium vacancies is 7.6 Å, and the FM state is found to be more stable than the AFM state by 112 meV, indicating a substantially long-range ferromagnetic ordering of cation vacancy induced by local magnetic moments in titanium-deficient TiO₂. As a result, it is proposed that the carriers, i.e., holes from the *p* orbitals of these oxygen ions, are thought to

induce the long-range ferromagnetism, and similar ferromagnetically coupled state is also expected in other cation-deficient semiconductors such as In_2O_3 , SnO_2 , and CdS .

In summary, first-principles GGA+U electronic structure calculations are carried out to investigate the magnetic property of oxygen-deficient anatase and rutile TiO_2 . Results of the calculations show that excess electrons introduced by an oxygen vacancy convert two Ti^{4+} ions into two Ti^{3+} ions and result in a local magnetic moment of about $1.0 \mu_B$ per Ti^{3+} ion in anatase phase. However, the two Ti^{3+} ions form a stable antiferromagnetic state. Similar antiferromagnetism also appears in oxygen-deficient rutile phase TiO_2 . The calculated results are consistent with the experimentally observed antiferromagnetic behavior in oxygen-deficient Ti-O system.

ACKNOWLEDGMENTS

This work is supported by the Singapore National Research Foundation Competitive Research Program (Grant No. NRF-G-CRP 2007-05), National Basic Research Program of China (973 program, Grant No. 2007CB613302), National Natural Science Foundation of China under Grant No. 10774091, Natural Science Foundation of Shandong Province under Grant No. Y2007A18, and the Specialized Research Fund for the Doctoral Program of Higher Education 20060422023.

E-mail addresses: daiy60@sina.com (Ying Dai^{*}), phyfyp@nus.edu.sg (Yuanping Feng[†])

References:

- ¹ Y. Matsumoto, et al., *Science* **291**, 854 (2001).
- ² K. R. Kittilstved, D. A. Schwartz, A. C. Tuan, S. M. Heald, S. A. Chambers, and D. R. Gamelin, *Phys. Rev. Lett.* **97**, 037203 (2006).
- ³ J. M. D. Coey, M. Venkatesan, P. Stamenov, C. B. Fitzgerald, and L. S. Dorneles, *Phys. Rev. B* **72**, 024450 (2005).
- ⁴ M. Venkatesan, C. B. Fitzgerald, and J. M. D. Coey, *Nature* **430**, 630 (2004).
- ⁵ J. M. D. Coey, *Solid State Sci.* **7**, 660 (2005).
- ⁶ C. DasPemmaraju and S. Sanvito, *Phys. Rev. Lett.* **94**, 217205 (2005).
- ⁷ N. H. Hong, J. Sakai, N. Poirot, and V. Brizé, *Phys. Rev. B* **73**, 132404 (2006).
- ⁸ N. H. Hong, N. Poirot, and J. Sakai, *Phys. Rev. B* **77**, 033205 (2008).
- ⁹ S. D. Yoon, Y. Chen, A. Yang, T. L. Goodrich, X. Zuo, D. A. Arena, K. Ziemer, C. Vittoria, and V. G. Harris, *J. Phys.: Condens. Matter* **18**, L355 (2006).
- ¹⁰ A. K. Rumaiz, B. Ali, A. Ceylan, M. Boggs, T. Beebe, and S. I. Shah, *Solid State Commun.* **144**, 334 (2007).
- ¹¹ A. Hassini, J. Sakai, J. S. Lopez, and N. H. Hong, *Phys. Lett. A* **372**, 3299 (2008).
- ¹² C. Sudakar, P. Kharel, R. Suryanarayanan, J. S. Thakur, V. M. Naik, R. Naik, and G. Lawes, *J. Magn. Magn. Mater.* **320**, L31 (2008).
- ¹³ Y. Bai and Q. Chen, *phys. stat. sol. (RRL)* **2**, 25 (2008).
- ¹⁴ H. Peng, J. Li, S.-S. Li, and J.-B. Xia, *Phys. Rev. B* **79**, 092411 (2009).
- ¹⁵ E. Finazzi, C. D. Valentin, G. Pacchioni, and A. Selloni, *J. Chem. Phys.* **129**, 154113 (2008).

- ¹⁶ G. Mattioli, F. Filippone, P. Alippi, and A. AmoreBonapasta, Phys. Rev. B **78**, 241201(R) (2008).
- ¹⁷ S. Zhou, et al., Phys. Rev. B **79**, 113201 (2009).
- ¹⁸ G. Kresse and J. Furthmuller, Comput. Mater. Sci. **6**, 15 (1996).
- ¹⁹ G. Kresse and J. Furthmuller, Phys. Rev. B **54**, 11169 (1996).
- ²⁰ J. P. Perdew, J. A. Chevary, S. H. Vosko, K. A. Jackson, M. R. Pederson, D. J. Singh, and C. Fiolhais, Phys. Rev. B **46**, 6671 (1992).
- ²¹ S. L. Dudarev, G. A. Botton, S. Y. Savrasov, C. J. Humphreys, and A. P. Sutton, Phys. Rev. B **57**, 1505 (1998).
- ²² V. I. Anisimov, J. Zaanen, and O. K. Andersen, Phys. Rev. B **44**, 943 (1991).
- ²³ C. J. Calzado, N. C. Hernández, and J. Sanz, Phys. Rev. B **77**, 045118 (2008).
- ²⁴ L. K. Keys and L. N. Mulay, Phys. Rev. **154**, 453 (1967).
- ²⁵ P. W. Anderson, Phys. Rev. **79**, 350 (1950).
- ²⁶ I. S. Elfimov, S. Yunoki, and G. A. Sawatzky, Phys. Rev. Lett. **89**, 216403 (2002).

Figure Captions

Figure 1 Total (a) and partial (b, and c) DOS plots of oxygen-deficient anatase TiO₂. The vertical dotted line indicates the Fermi level.

Figure 2 Total (a) and partial (b, and c) DOS plots of oxygen-deficient rutile TiO₂. The vertical dotted line indicates the Fermi level.

Figure 3 Partial geometrical structures of the models for oxygen-deficient (a) anatase and (b) rutile TiO₂. The larger gray and small red spheres represent the Ti and O atoms respectively, and the white spheres show the position of oxygen vacancies.

Figure 4 Spin densities around the oxygen vacancy in anatase (a) and rutile (b) TiO₂ under antiferromagnetic alignment. Yellow and cyan isosurfaces correspond to up- and down-spin densities, respectively.

Figure 5 Schematic of the AFM coupling between the two Ti³⁺ ions around the oxygen vacancy.

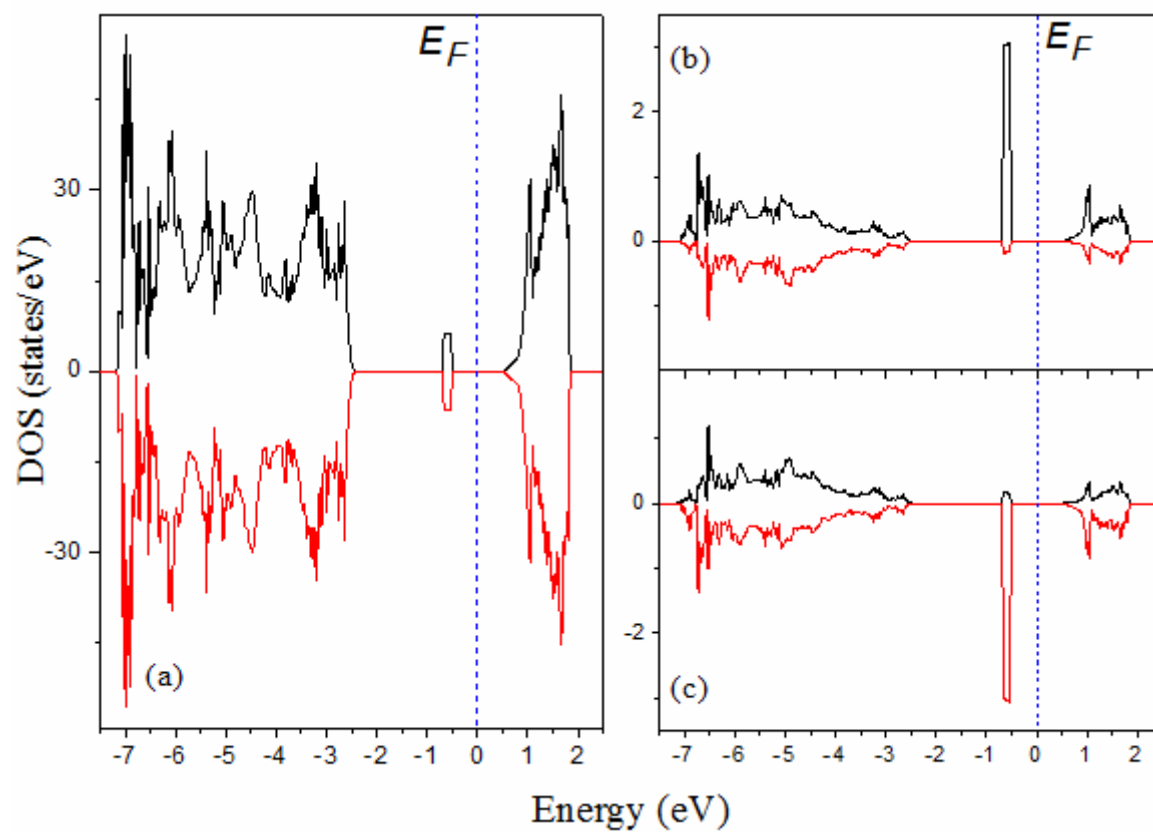


Figure 1

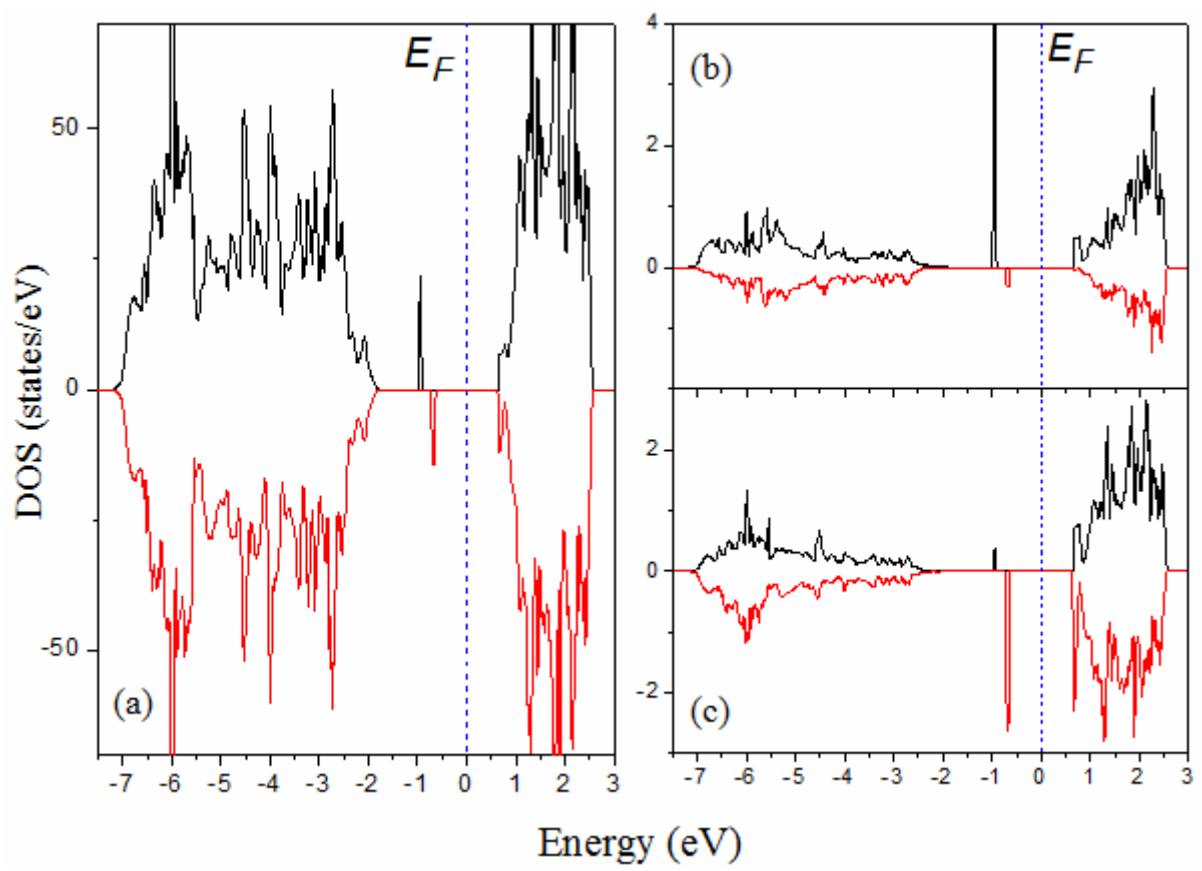


Figure 2

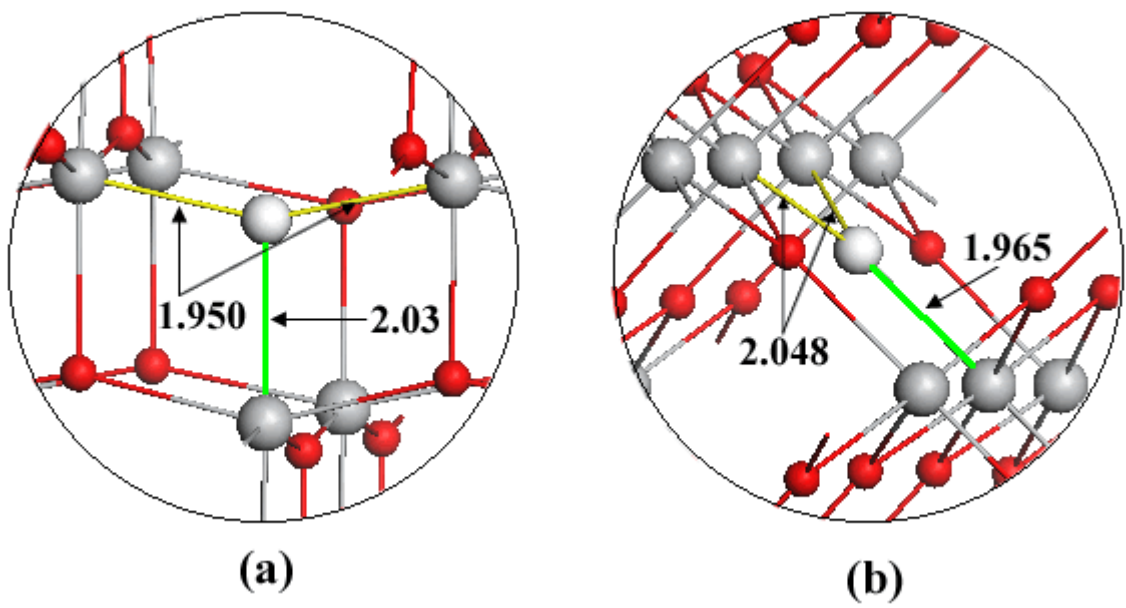


Figure 3

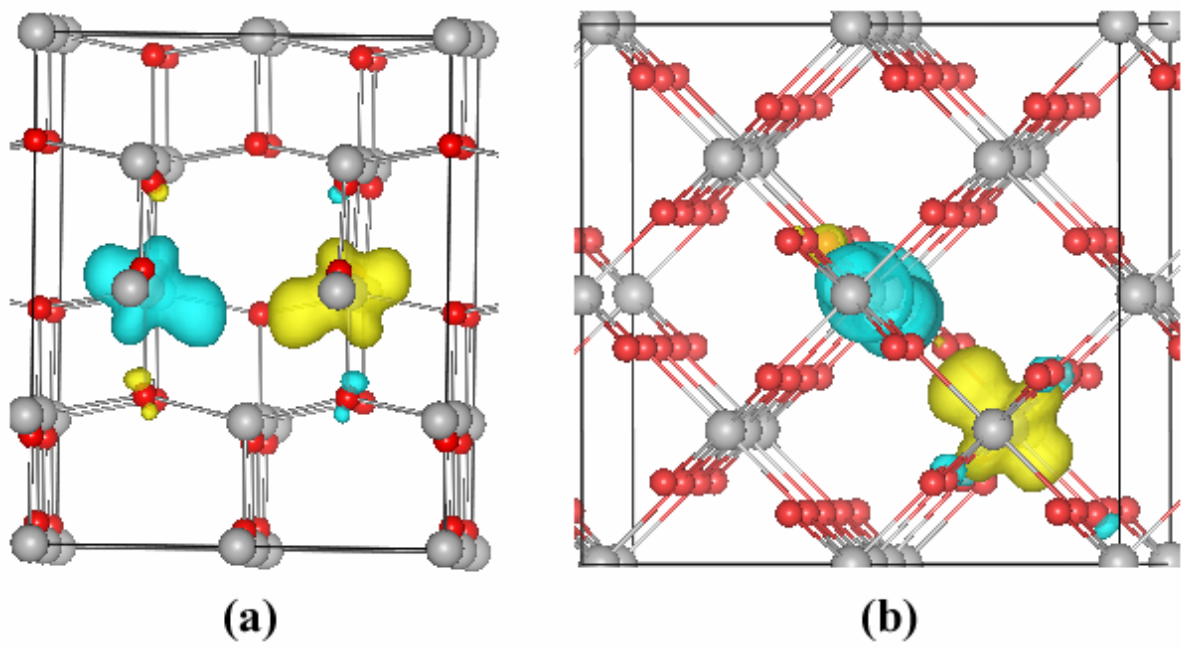


Figure 4

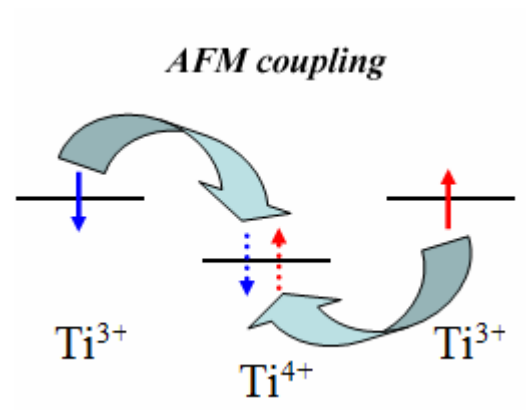


Figure 5